A SENSITIVE NANOSENSOR FOR THE *IN SITU* DETECTION OF THE CANNIBAL DRUG

Eva Garrido, [†,‡,¥,§] María Alfonso, [†,¥,§] Borja Díaz de Greñu, [†,‡,¥,§] María Dolores Marcos,[†,‡,¥,§,#] Ana M. Costero,[†,‡,Δ] Salvador Gil,[†,‡,Δ] Félix Sancenón,*[,†,‡,¥,§,#] and Ramón Martínez-Máñez*[,†,‡,¥,§,#]

[†] Instituto Interuniversitario de Investigación de Reconocimiento Molecular y Desarrollo Tecnológico (IDM), Universitat Politècnica de València, Universitat de València, Spain.

[‡] CIBER de Bioingeniería, Biomateriales y Nanomedicina (CIBER-BBN).

[¥] Unidad Mixta UPV-CIPF de Investigación en Mecanismos de Enfermedades y Nanomedicina, Universitat Politècnica de València, Centro de Investigación Príncipe Felipe, Valencia, Spain.

[§] Unidad Mixta de Investigación en Nanomedicina y Sensores. Universitat Politècnica de València, Instituto de Investigación Sanitaria La Fe, Valencia, Spain.

[#] Departamento de Química, Universitat Politècnica de València, Camino de Vera s/n, 46022, Valencia, Spain.

[Δ] Departamento de Química Orgánica, Facultad de Química, Universitat de València, Doctor Moliner 50, 46100, Valencia, Spain.

KEYWORDS. Nanosensor, mesoporous silica nanoparticles, MDPV, Cannibal drug, recombinant human dopamine transporter (DAT).

ABSTRACT: A bio-inspired nanodevice for the selective and sensitive fluorogenic detection of 3,4-methylenedioxypyrovalerone (MDPV), usually known as Cannibal drug, is reported. The sensing nanodevice is based on mesoporous silica nanoparticles (MSNs), loaded with a fluorescent reporter (rhodamine B) and functionalized on their external surface with a dopamine derivative (**3**), which specifically interacts with the recombinant human dopamine transporter (DAT), capping the pores. In the presence of MDPV, DAT detaches from the MSNs consequently causing rhodamine B release and allowing drug detection. The nanosensor shows a detection limit of 5.2 μM and it is able to detect the MDPV drug both in saliva and blood plasma samples.

Over the last years, the unprecedented growth in the number of new psychoactive substances (NPS) globally available and the expansion of a more dynamic illegal market for these drugs is causing a great threat to public safety. Regarding last studies published, an estimated 271 million people worldwide had used psychoactive drugs at least once during 2019; roughly 5.5 % of the global population.[1, 2] Moreover, psychostimulants have reached popularity as potent abuse drugs.[3] Among NPS, synthetic cathinones have arisen as the most widespread class designed drugs. This new group of recreational drugs, commonly known as "bath salts", "legal highs", "plant food" or "research chemicals", acts improving the function of the three main monoamine neurotransmitters: i.e. dopamine, norepinephrine and serotonin.[4, 5] With regard to physical forms, cathinones are odourless, white or brownish solids, commonly presented in the illegal market as powders or fine crystals, and less frequently as tablets or capsules.[6, 7] Main administration routes reported of cathinones are insufflation (snorting), oral ingestion (the substance is diluted in water or juice drink), and "bombing" (wrapping powders in a cigarette paper and next swallowed).[8]

Structurally, cathinones are β-ketone derivatives of psychoactive phenylalkylamine alkaloids; a naturally occurring stimulant in the khat plant (*Catha edulis*). One of the most remarkable constituents of the cathinones family is 3,4-methylenedioxypyrovalerone (MDPV). MDPV is popularly known as "Cannibal drug", because, when taken in high doses, it spurs users into violent outbreaks of aggression, paranoia and panic attacks.[9] MDPV differs from other synthetic cathinones in the fact that it contains a pyrrolidine ring, which gives the drug potent actions as an uptake blocker of dopamine and norepinephrine transporters. When consumed, MDPV links to the dopamine active transporter (DAT), blocking dopamine reuptake out of the synaptic cleft. In this way, MDPV leads to a rise in the extracellular dopamine levels, causing a powerful locomotive enhancement even ten times more potent than that produced by cocaine.[10-12] Moreover, MDPV potentially produces some adverse effects derived from long-lasting psychostimulant-type toxidrome, including severe agitation, violent behavior, tachycardia, psychosis, profuse diaphoresis, paranoia and anxiety, among others. Currently reported intoxications involving MDPV[13, 14] stablished that the amount of synthetic cathinones consumed per dose ranged from 5 to 250 mg orally which produced effects lasting from 1 to 3 h.[15]

MDPV is commonly detected by different techniques such as HPLC-MS,[16-19] GC-MS,[20-22] HPIMS,[23] and bioanalytical procedures.[24-26] Nevertheless, these methods are slow, the samples must be moved to qualified laboratories and they usually require the supervision of trained personnel. An alternative promising approach to these techniques involves the development of chromo-

fluorogenic sensors for the rapid, selective and '*in-situ*' detection of MDPV.[27] However, as far as we know, no chromo-fluorogenic probes have been reported for the detection of MDPV so far. In this scenario, the development of new strategies to detect and quantify "drugs of abuse" like MDPV in a fast, easy, and reliable way is timely and urgently required.

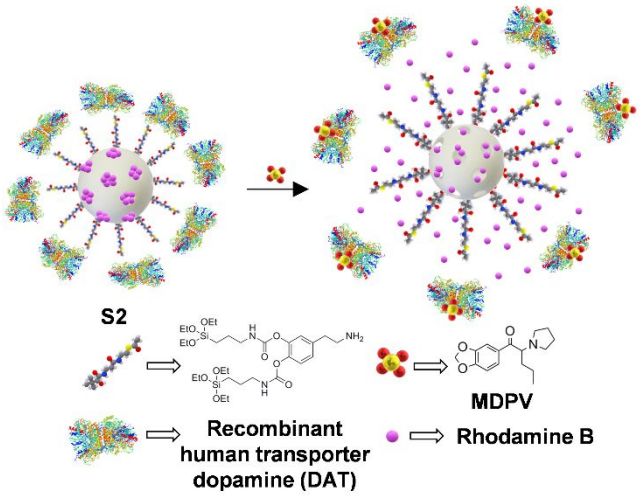

Scheme 1. Sensing behavior of solid **S2** in the presence of MDPV.

From another point of view, the development of hybrid organic-inorganic gated materials based on mesoporous silica nanoparticles (MSNs) with applications in drug delivery,[28,29] communication[30,31] and detection protocols[32-34] has attracted great attention over the last decade. The main advantages provided by MSNs are high specific surface area, homogeneous porosity, high load capacity, tunable pore size (2-10 nm) and easy functionalization. These sensing gated materials allow the controlled release of an entrapped cargo in the presence of a target molecule, usually triggering the displacement of the gating ensemble.[35] Moreover, these capped sensing materials also show inherent chemical amplification as only few molecules of the analyte can induce the delivery of a large amount of the entrapped cargo (usually a fluorophore).[36]

Based on the above, we report herein a gated nanodevice for the selective, sensitive fluorogenic sensing of MDPV (Scheme 1). The sensor selectively detects MDPV at concentrations as low as 5.2 μM and is able to determine the presence of MDPV both in saliva and blood plasma.

EXPERIMENTAL SECTION

Synthesis of mesoporous silica nanoparticles. NaOH (2.00 mol L^{-1}, 3.5 mL) was added to a solution of CTABr (1.00 g, 2.74 mmol) in deionized H_2O (480 mL) at 40 °C. The solution temperature was adjusted to 80 °C and then TEOS (5.00 mL, 2.57 × 10^{-2} mol) was added dropwise. The mixture was stirred for 2 h to give a white precipitate. The solid was isolated by centrifugation and washed with deionized water and then dried at 70 °C for 12 h. In order to remove the template phase, the mesoporous nanoparticles were calcined at 550 °C for 5 h in an oxidizing atmosphere.

Synthesis of tert-butyl (3,4-dihydroxyphenethyl)carbamate (2)[37]. Dopamine hydrochloride (**1**, 1.00 g, 6.53 mmol) was suspended in 13 mL of chloroform and then, sodium bicarbonate (0.55 g, 6.53 mmol) in 9 mL of H_2O, NaCl (1.31 g, 22 mmol) and di-tert-butyl dicarbonate (1.49 g, 6.83 mmol) were successively added. The mixture was heated at 62 °C for 3 h. Afterwards, the organic phase was washed with H_2O (40 mL), brine (40 mL), dried over $MgSO_4$, and filtered. Finally, the filtrate was concentrated by rotary evaporation and the residue was purified by silica gel column chromatography using ethyl acetate-hexane as eluent (1:1 v/v) to obtain the product **2** as a pale pink solid (921 mg, 3.64 mmol, 56 % yield). (Scheme 2a).

Synthesis of 4-(2-((tert-butoxycarbonyl)amino)ethyl)-1,2-phenylene bis((3-(triethoxysilyl)propyl)carbamate) (3): In a reaction vessel purged with Argon, a solution of **2** (0.3 g, 1.18 mmol) in 15 mL of anhydrous CH_3CN was prepared, and then (3-isocyanatopropyl)-triethoxysilane (0.6 mL, 2.36 mmol) was added. The mixture was stirred at room temperature for 4 h. Finally, the solvent was removed under reduced pressure to obtain product **3** as a pale yellow solid (882.6 mg, 1.18 mmol). ^{1}H-NMR (400 MHz, $CDCl_3$) δ 7.09 (d, *J*=8.2 Hz, 1H), 6.99 (d, *J*=7.3 Hz, 2H), 5.47 (s, 2H), 4.58 (s, 1H), 3.83 (qdd, J_1=7.0, J_2=5.0, J_3=2.0 Hz, 15H), 3.36 (d, *J*=5.7 Hz, 2H), 2.77 (t, *J*=6.7, 2H), 1.43 (s, 11H), 1.23 (m, 25H) ppm. ^{13}C-NMR (101 MHz, $CDCl_3$) δ 157.05, 154.67, 152.89, 141.79, 140.38, 136.03, 125.16, 122.5, 77.99, 57.25, 42.47, 41.75, 40.27, 34.31, 27.18, 22.39, 21.94, 17.07, 6.41 ppm. (Figure S1-S2)

Synthesis of S1-Boc. In a typical synthesis, a mixture of calcined mesoporous silica nanoparticles (100 mg) and rhodamine B (38.3 mg, 0.08 mmol) were suspended in 5 mL of anhydrous CH_3CN and purged with Argon. The suspension was stirred at room temperature for 24 h in order to load the mesopores. Then, compound **3** (191.5 mg, 0.26 mmol) was added and the final suspension was stirred at room temperature for 5.5 h. Finally, the resulting pink solid was filtered and then dried under vacuum overnight, giving rise to **S1-Boc** (195 mg).

Synthesis of S1. Solid **S1-Boc** (10 mg) was suspended in 2 mL of anhydrous CH_2Cl_2 and purged with Argon. The suspension was then cooled to 0 °C and TFA (0.1 mL, 1.31 mmol) was added for N-Boc deprotection. The mixture was stirred at room temperature for 10 minutes and the solid was isolated by centrifugation, washed with CH_2Cl_2 (2 × 8 mL) and dried overnight at 37 °C.

Synthesis of S2. Solid **S1** (1 mg) was suspended in TRIS HCl buffer (300 μL, 20 mM of TRIS and $MgCl_2{\cdot}6H_2O$, pH 8.0) and then, the recombinant human transporter dopamine protein (150 μL, 0.017 μg/μL) was added. The mixture was stirred in a thermo-shaker at 4 °C overnight. Then, the suspension was centrifuged at 12,000 rpm for 5 min. **S2** was then washed with TRIS HCl buffer (300 μL) to eliminate the non-encapsulated dye and the unattached protein.

Release experiments of solid S1 in the presence of MDPV. To check the crucial role played by transporter dopamine protein (DAT), absent in **S1** but present in **S2**, 1 mg of solid **S1** was suspended in 800 μL of TRIS HCl buffer and this volume was divided into two aliquots of 400 μL.

After that, 9 µL of a 20 mM solution of MDPV in TRIS HCl buffer were added to one of the aliquots (final concentration of 860 µM), and simultaneously, 9 µL of TRIS HCl buffer were added to the blank aliquot. Both suspensions were stirred at 25 °C and, after certain time, aliquots were centrifuged (12,000 rpm for 5 min) and the fluorescence of the rhodamine B released in the supernatant (λ_{exc} = 565 nm, λ_{em} = 572 nm) was measured. Once measured, the 150 µL were returned to the initial suspension (Figure S9).

Release experiments of solid S2 in the presence of MDPV. The same procedure described in the section above was carried out with **S2** (Figure 1).

Selectivity studies with S2 in TRIS buffer. 1 mg of **S2** was suspended in 1.4 mL of TRIS HCl Buffer (20 mM of TRIS and $MgCl_2{\cdot}6H_2O$, pH 8.0) and this volume was separated into seven aliquots of 200 µL. Besides, several solutions in TRIS HCl buffer of different drugs (MDMA, morphine, heroin, cocaine, MDPV, and dopamine) at a concentration of 1 mM were prepared. Then, 9 µL of each drug solution were added to the aliquots of **S2**, to reach a final concentration of 43 µM. Simultaneously, 9 µl of TRIS HCl buffer were added to the blank. The suspensions were stirred at 25 °C for 2 minutes. After that, the aliquots were centrifuged, and the fluorescence of the rhodamine B released in the supernatant was measured (Figure 2).

Determination of detection limit of S2 for MDPV. 1 mg of **S2** was suspended in 2.4 mL of TRIS HCl buffer (20 mM of TRIS and $MgCl_2{\cdot}6H_2O$, pH 8.0) and then divided into twelve aliquots of 200 µL. Then different concentrations of MDPV were added to the aliquots. The suspensions were stirred at 25 °C for 2 min and then centrifuged (12,000 rpm for 5 min) and the fluorescence of the rhodamine B released in the supernatant (λ_{exc} = 565 nm, λ_{em} = 572 nm) was measured (Figure S10).

Determination of detection limit of S2 with MDPV in saliva. 1 mg of **S2** was suspended in 2.4 mL of 30 % saliva and divided into twelve aliquots of 200 µL each one. The experimental procedure followed was the same as described above (Figure S14).

Determination of detection limit of S2 with MDPV in blood plasma. 1 mg of **S2** was suspended in 2.4 mL of 30 % diluted blood plasma extracted and divided into twelve aliquots of 200 µL. The experimental procedure is the same as described above (Figure S15).

Detection of MDPV in spiked saliva and plasma blood samples. 0.1 mg of solid **S2** were added to 200 µL of 30 % saliva or plasma sample spike with MDPV. All suspensions were stirred at 25 °C for 2 minutes. The aliquots were centrifuged (12,000 rpm for 5 min) and the fluorescence of the rhodamine B released in the supernatant (150 µL) was measured (Figure S11-S13).

RESULTS AND DISCUSSION

Design, synthesis and characterization of the nanodevice. For the preparation of the sensing nanoparticles, MSNs was first synthesized by base-catalysed sol–gel condensation of tetraethylorthosilicate (TEOS) in the presence of sodium hydroxide and hexadecyltrimethylammonium bromide (CTABr) as micellar template, following previously reported procedures.[38,39] The as-made MSNs were calcined at 550 °C to obtain the starting nanoparticles. In a second step, the pores of the MSNs were loaded with rhodamine B by stirring a suspension of nanoparticles in a concentrated acetonitrile solution of the fluorophore (**S0**). Furthermore, dopamine derivative **3** was anchored onto the external surface of the loaded nanoparticles yielding the solid **S1-Boc**. Synthesis of **3** was carried out by protecting the amino group of dopamine with di-tert-butyl dicarbonate following with reaction with (3-isocyanatopropyl)triethoxysilane. The Boc protecting groups from **S1-Boc** were removed by using trifluoroacetic acid (TFA), giving rise to solid **S1** (Scheme 2b). The final sensing nanodevice (**S2**) was obtained after stirring a suspension of **S1** in TRIS HCl buffer at pH 8.0 and the DAT protein overnight.

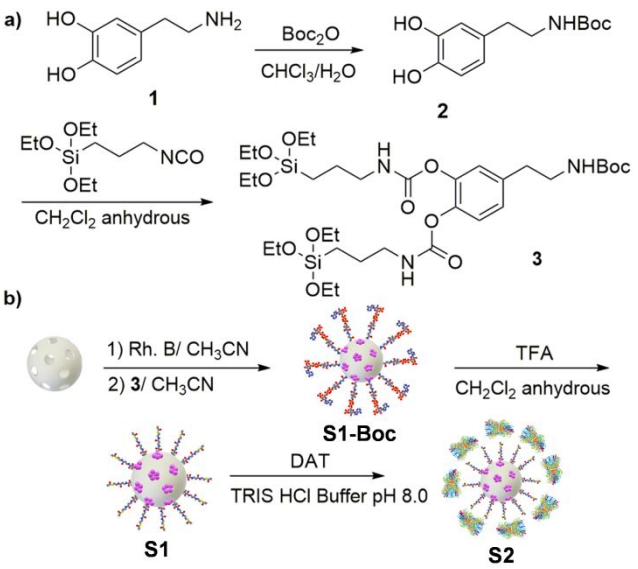

Scheme 2. (a) Synthesis of dopamine derivative **3**. (b) Synthetic route for the preparation of solid **S2**.

All the prepared solids were characterized by using standard techniques such as powder X-ray diffraction (PXRD), transmission electron microscopy (TEM), N_2 adsorption–desorption isotherms, elemental and thermogravimetric analyses, dynamic light scattering (DLS) and FTIR (Figures S3-S8). In particular, the PXRD pattern of the MSNs as synthesized (Figure S3, curve a) shows four low-angle reflections typical of a hexagonal array, indexed as (1 0 0), (1 1 0), (2 0 0), and (2 1 0) Bragg peaks. Besides a cell parameter a_0 of 39.75 Å (distance between planes d_{100} = 34 Å) was determined. A significant displacement of 6-8 Å of the (1 0 0) peak in the PXRD pattern of the MCM-41 calcined nanoparticles is evident in curve b (Figure S3), related to the condensation of silanol groups in the calcination step. In **S1**, a broadening of the (1 1 0) and (2 0 0) reflections is observed, related to a loss of contrast due to filling of the pore with rhodamine B. The presence of the mesoporous structure in the final functionalized solids was also confirmed by TEM analyses, in which the typical hexagonal porosity of a MCM-41-like matrix was clearly visualized (Figure S4). The figure also shows that the materials are spherical particles with an

average diameter of 100 ± 4 nm (for **S2**, n = 100 particles). The N_2 adsorption–desorption isotherms of the calcined nanoparticles show a IV type isotherm, typical of mesoporous materials (Figure S5). The curve increment at P/P_0 value (0.2–0.4) is ascribed to the condensation of nitrogen by capillarity inside the mesopores. A pore diameter of 2.54 nm and a total pore volume of 0.90 cm^3 g^{-1} were calculated by using the BJH model on the adsorption branch of the isotherm. The application of the Brunauer-Emmett-Teller (BET) model resulted in a value for the total specific surface of 1129 m^2 g^{-1}. The N_2 adsorption–desorption isotherm of **S1-Boc** (Figure S5) is typical of mesoporous systems with partially filled mesopores. A decrease in the pore volume (0.20 cm^3 g^{-1}) and surface area (318.48 m^2 g^{-1}) was observed. From thermogravimetric (Figure S6), elemental analysis and delivery studies, contents of 0.3 and 0.19 mmol of rhodamine B and **3**, respectively per gram of **S1-Boc** solid were calculated. Moreover, contents of 0.07 and 0.16 mmol of rhodamine B and **3**, respectively per gram of **S1** solid were determined. Meanwhile, the zeta potential of -29.5 mV, in the starting MSNs, changed to 22.4 mV for **S1-Boc**, due to attachment of the dopamine derivative, **3**. Besides, solid **S1** presents a potential z value of 29.1 mV because of deprotection of amino group, whereas a value of -38.0 mV was found for solid **S2** on account of the DAT attachment. Additionally, the hydrodynamic diameter of the starting MSNs was 159 ± 1 nm. **S1-Boc** presented a hydrodynamic diameter of 238 ± 9 nm, which changed to197 ± 2 nm for **S1** (Figure S7). This decrease in size is in agreement with the removal of the protective Boc groups from **S1-Boc** to give **S1**. Finally, the hydrodynamic diameter for **S2** increased to 501 ± 13 nm due to the attachment of the DAT protein. FTIR spectrum of functionalized solid **S1** showed the typical absorption bands at ca. 1100 and 3400 cm^{-1} related to the bond stretching vibrations of Si-O-Si and of O-H groups respectively. In addition, the spectrum showed the stretching N-H vibrations of amine groups at 3300 cm^{-1}, which were not present in FTIR spectrum of solid **S1-Boc** (Figure S8). **S2** showed absorption bands at ca. 3300, 1760 and 1500 cm^{-1} related to the vibrations of N-H, C=O and NH_3^+ respectively.

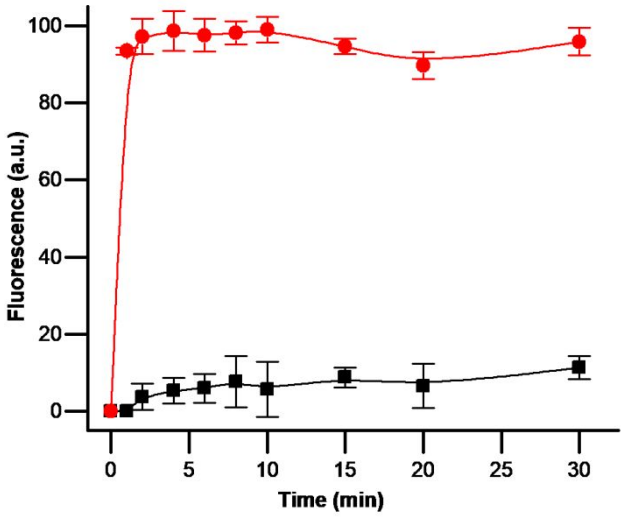

Figure 1. Kinetics of dye release from solid **S2** in TRIS HCl Buffer at pH 8.0 in absence (black line) and in presence (red line) of MDPV (860 μM). Error bars are expressed as 3σ for three independent experiments.

Controlled delivery studies. To assess the feasibility of the proposed sensing paradigm, controlled release experiments from **S2** in the presence of MDPV were carried out. For this purpose, **S2** was suspended in TRIS HCl buffer at pH 8.0 and this volume was divided into two aliquots. Then, a solution of MDPV in TRIS HCl buffer were added to one of the aliquots (MDPV final concentration of 860 μM), and simultaneously, TRIS buffer was added to the blank aliquot. Both suspensions were stirred at 25 °C and, after predefined times, aliquots were taken and centrifuged to eliminate the solid and the fluorescence of the rhodamine B released in the supernatant (λ_{exc} = 565 nm, λ_{em} = 572 nm) was measured. The obtained release profiles are shown in Figure 1. As can be seen, in the absence of MDPV a low cargo delivery (ca. 7 % of the total rhodamine B released after 20 min) was observed, indicating that **S2** was effectively capped by the interaction of the grafted dopamine derivative with DAT. However, in the presence of MDPV, a remarkable enhancement in the fluorescence emission at 572 nm was detected, as a consequence of the selective coordination of the drug with DAT, which resulted in DAT displacement from the solid, pore opening and rhodamine B release. These results are consistent with the fact that MDPV shows high affinity for DAT in the low nanomolar range (10 ± 2 nM) compared to the low affinity presented for other transporters such as serotonin (2.86 ± 0.1 μM)[40] Likewise, MDPV produces a highly potent DAT inhibition with an IC_{50} value of 4.1 ± 0.5 nM in contrast to the weak effect produced by serotonin and norepinephrine transporters (IC_{50} = 3349 ± 305 and 26 ± 8 nM, respectively).[41, 42] Besides, in order to demonstrate that DAT plays a key role in the gating mechanism, we measured the delivery profiles of the uncapped solid **S1** in absence and presence of MDPV (Figure S9). In both cases, a marked rhodamine B release was observed.

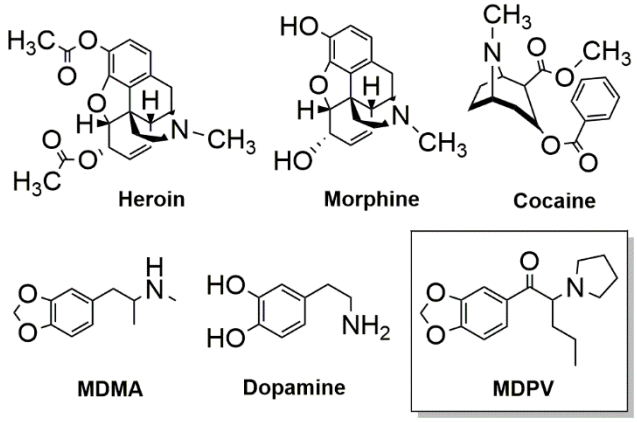

Scheme 3. Chemical structure of the drugs used as interferents for selectivity studies.

To study the sensitivity of **S2** towards MDPV, the fluorogenic response of TRIS HCl buffer suspensions of the nanodevices upon addition of increasing amounts of the drug was studied (Figure S10). The results showed an increase in the rhodamine B emission at 572 nm after 2 min upon addition of increasing concentrations of MDPV.

From the titration profile, a detection limit for MDPV of 5.2 μM was determined from the intersection between two linear sections of the calibration curve. The detection limit achieved enables a commonly occurring dose of MDPV (5 mg) to be detected in volumes as high as 3.5 L.

In a further step, the fluorogenic response of **S2** was also evaluated in the presence of other common drugs such as cocaine, heroin, dopamine, MDMA, and morphine (Scheme 3). Figure 2 shows the emission of the released rhodamine B at 572 nm after 2 min from suspensions of **S2** in TRIS HCl buffer at pH 8.0 upon addition of the selected drugs (1 mM). As can be seen, a remarkable enhancement in the fluorescence intensity is only produced by MDPV, while other drugs were unable to induce such a remarkable change. The observed selectivity of **S2** toward MDPV is in agreement with its higher IC_{50} inhibition value (4.1 ± 0.5 nM) to DAT compared to other tested drugs such as cocaine or MDMA (IC_{50} = 211 ± 19 and 93 ± 17, respectively).[41] Therefore, none of the other interferents tested presented remarkable affinities with DAT and, as a consequence, negligible rhodamine B release was observed in these cases. This suggested that **S2** could be used for the selective detection of MDPV.

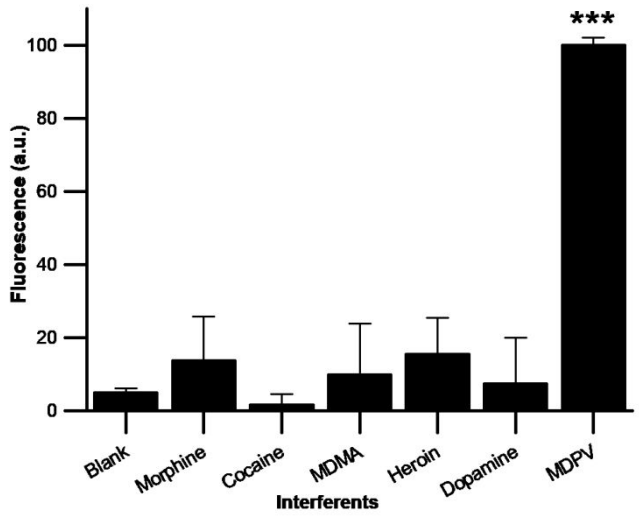

Figure 2. Effect of the indicated drugs (1 mM) on the relative rhodamine B release from solid **S2** in TRIS HCl buffer at pH 8.0 20 min after addition. Error bars are expressed as 3σ for three independent experiments (***p<0.0003).

Validation studies in realistic samples. In order to evaluate the applicability of the nanosensor in realistic competitive environments, we tested the ability of **S2** to detect MDPV in real samples of both saliva and blood plasma. In this way, we prepared a solution of 30 % saliva and then the release of rhodamine B from **S2** nanoparticles in the presence (860 μM) and absence of the drug was measured. The results obtained (Figure S11) showed that while in absence of MDPV a moderate dye release was found (15 % of the total dye released after 30 min), in the presence of the illicit drug a marked rhodamine B release was produced (98 % after ca. 30 min). Moreover, the sensitivity of **S2** in saliva was measured, showing a detection limit for MDPV of 6.9 μM (Figure S14).

In addition, we tested the ability of **S2** to detect MDPV in a solution of 30 % blood plasma previously spiked with MDPV (860 μM) (Figure S12). As shown in the Figure S13 rhodamine B release was observed when the drug was present in blood plasma solution (98 % of dye released after 20 min), while the nanoparticles remained "closed" when no MDPV was present, and the fluorescence emission was significantly lower (20 % after ca. 20 min). The detection limit of MDPV in blood plasma for **S2** was as low as 12.1 μM (Figure S15). Detection limit values obtained in saliva and in plasma are slightly higher than that measured in TRIS HCl solution (*vide ante*), most probably due to the presence of a higher competitive environment.

Finally, the nanosensor was tested for MDPV detection in saliva and blood plasma samples (200 μL) spiked with 17.9 and 215 μM of the cannibal drug, respectively. 0.1 mg of solid **S2** was added to the corresponding solution and the samples were shaken for 2 minutes at room temperature. From the interpolation in calibration curves of the rhodamine released from **S2** in these media, concentrations of MDPV of 17.6 and 200 μM were determined for the saliva and plasma samples, respectively (recovery values of 98 % and 93 %).

CONCLUSIONS

In summary, we report herein the design, synthesis, characterization and sensing behaviour of a probe for the fast and highly selective detection of the cathinone MDPV (cannibal drug). The nanosensor consists of MSNs loaded with rhodamine B and capped with DAT. In the presence of the MDPV drug, DAT is detached from the nanosensor, inducing cargo release. This behaviour is observed in the presence of MDPV but not with other common drugs like cocaine, morphine, heroin, heroin or MDMA. The probe shows a high sensitivity in TRIS HCl buffer (detection limit of 5.2 μM) and in realistic competitive media like saliva (6.9 μM) and blood plasma (12.1 μM). Finally, the probe is able to detect MDPV in spiked saliva and serum samples. Considering the sensitivity and selectivity of **S2** and its easy synthesis and handling, this material could be used as a reliable system for the accurate '*in situ*' and '*at site*' MDPV identification.

ASSOCIATED CONTENT

Supporting Information. Materials and methods, experimental details about solid synthesis **S2**, ^{1}H-NMR and ^{13}C-NMR of compound **3**, characterization images and graphs, control release experiments in TRIS Buffer, saliva and blood plasma and calibration curves in aqueous media, saliva and blood plasma. "This material is available free of charge via the Internet at http://pubs.acs.org."

AUTHOR INFORMATION

Corresponding Author

* E-mail: rmaez@qim.upv.es.

Author Contributions

The manuscript was written through contributions of all authors. All authors have given approval to the final version of the manuscript. E.G., M.A., B.D.G. and R.M.M. conceived and designed the research, performed most of the experiments, contributed to the experimental designs, data analysis,

discussion and writing. E.G., M.A., B.D.G., S.G. and F.S. synthesized and characterized all organic molecules. E.G., M.A. and M.D.M. carried out the synthesis and characterization of the sensory material. E.G. carried out the controlled release studies and determined the sensing features of the nanoparticles. E.G., M.A., A.M.C. and R.M.M. analyzed the data. Finally, E.G., A.M.C., S.G., F.S. and R.M.M. wrote the manuscript with feedback from all the authors.

Notes

The authors declare no competing financial interest.

ACKNOWLEDGMENT

The authors thank the Spanish Government (projects RTI2018-100910-B-C41 (MCUI/AEI/FEDER, UE) and CTQ2017-87954-P) and the Generalitat Valencia (PROMETEO/2018/024) for support. E. G. is grateful to the Spanish MEC for her FPU grant. M. A. thanks to her postdoctoral fellowship (PAID-10-17). The authors also thank the Electron Microscopy Service at the UPV for support.

REFERENCES

(1) World drug report. United Nations Office on Drugs and Crime (UNODC). Inform **2019**.

(2) European drug report: Trends and Developments. European Monitoring Centre for Drugs and Drug Addition (EMCDDA). Inform **2019**.

(3) New Psychoactive Substances: Pharmacology, Clinical, Forensics and Analytical Toxicology. Handbook of Experimental Pharmacology. *Springer* **2004**, *252*.

(4) Zawilska, J. B.; Wojcieszak, J., Designer cathinones—An emerging class of novel recreational drugs. *Forensic Sci. Int.* **2013**, *231*, 42-53.

(5) Coppola, M.; Mondola, R., 3,4-Methylenedioxypyrovalerone (MDPV): Chemistry, pharmacology and toxicology of a new designer drug of abuse marketed online. *Toxicol. Lett.* **2012,** *208*, 12-15.

(6) Coppola, M.; Mondola, R., Synthetic cathinones: Chemistry, pharmacology and toxicology of a new class of designer drugs of abuse marketed as bath salts or plant food. *Toxicol. Lett.* **2012,** *211*, 144-149.

(7) Oliver, C. F.; Palamar, J. J.; Salomone, A.; Simmons, S. J.; Philogene-Khalid, H. L.; Stokes-McCloskey, N.; Rawls, S. M., Synthetic cathinone adulteration of illegal drugs. *Psychopharmacology* **2019,** *236*, 869-879.

(8) Riley, A. L.; Nelson, K. H.; To, P.; López-Arnau, R.; Xu, P.; Wang, D.; Wang, Y.; Shen, H.-W.; Kuhn, D. M.; Angoa-Perez, M.; Anneken, J. H.; Muskiewicz, D.; Hall, F. S., Abuse potential and toxicity of the synthetic cathinones (i.e., "Bath salts"). *Neurosci. Biobeha. Rev.* **2020**, *110*, 150-173.

(9) Ibáñez, M.; Pozo, Ó. J.; Sancho, J. V.; Orengo, T.; Haro, G.; Hernández, F., Analytical strategy to investigate 3,4-methylenedioxypyrovalerone (MDPV) metabolites in consumers' urine by high-resolution mass spectrometry. *Anal. Bioanal. Chem.* **2016,** *408*, 151-164.

(10) Colon-Perez, L. M.; Pino, J. A.; Saha, K.; Pompilus, M.; Kaplitz, S.; Choudhury, N.; Jagnarine, D. A.; Geste, J. R.; Levin, B. A.; Wilks, I.; Setlow, B.; Bruijnzeel, A. W.; Khoshbouei, H.; Torres, G. E.; Febo, M., Functional connectivity, behavioral and dopaminergic alterations 24 hours following acute exposure to synthetic bath salt drug methylenedioxypyrovalerone. *Neuropharmacology* **2018,** *137*, 178-193.

(11) Eshleman, A. J.; Nagarajan, S.; Wolfrum, K. M.; Reed, J. F.; Swanson, T. L.; Nilsen, A.; Janowsky, A., Structure-activity relationships of bath salt components: substituted cathinones and benzofurans at biogenic amine transporters. *Psychopharmacology* **2019,** *236*, 939-952.

(12) Glennon, R. A.; Young, R., Neurobiology of 3,4-methylenedioxypyrovalerone (MDPV) and α-pyrrolidinovalerophenone (α-PVP). *Brain Res. Bull.* **2016,** *126*, 111-126.

(13) Kraemer, M.; Boehmer, A.; Madea, B.; Maas, A., Death cases involving certain new psychoactive substances: A review of the literature. *Forensic Sci. Int.* **2019,** *298*, 186-267.

(14) Liveri, K.; Constantinou, M. A.; Afxentiou, M.; Kanari, P., A fatal intoxication related to MDPV and pentedrone combined with antipsychotic and antidepressant substances in Cyprus. *Forensic Sci. Int.* **2016,** *265*, 160-165.

(15) Marinetti, L. J.; Antonides, H. M., Analysis of synthetic cathinones commonly found in bath salts in human performance and postmortem toxicology: method development, drug distribution and interpretation of results. *J. Anal. Toxicol.* **2013,** *37*, 135-146.

(16) Freni, F.; Bianco, S.; Vignali, C.; Groppi, A.; Moretti, M.; Osculati, A. M. M.; Morini, L., A multi-analyte LC–MS/MS method for screening and quantification of 16 synthetic cathinones in hair: Application to postmortem cases. *Forensic Sci. Int.* **2019,** *298*, 115-120.

(17) Peiró Mde, L.; Armenta, S.; Garrigues, S.; de la Guardia, M., Determination of 3,4-methylenedioxypyrovalerone (MDPV) in oral and nasal fluids by ion mobility spectrometry. *Anal. Bioanal. Chem.* **2016**, *408*, 3265–3273.

(18) Cheng, S.-Y.; Ng-A-Qui, T.; Eng, B.; Ho, J., Detection of cathinone and mephedrone in plasma by LC-MS/MS using standard addition quantification technique. *J. Anal. Sci. Technol.* **2017**, *8*, 19-25.

(19) Glicksberg, L.; Bryand, K.; Kerrigan, S., Identification and quantification of synthetic cathinones in blood and urine using liquid chromatography-quadrupole/time of flight (LC-Q/TOF) mass spectrometry. *J. Chromatogr. B* **2016**, *1035*, 91-103.

(20) Mercieca, G.; Odoardi, S.; Cassar, M.; Strano Rossi, S., Rapid and simple procedure for the determination of cathinones, amphetamine-like stimulants and other new psychoactive substances in blood and urine by GC–MS. *J. Pharm. Biomed. Anal.* **2018,** *149*, 494-501.

(21) Gerace, E.; Caneparo, D.; Borio, F.; Salomone, A.; Vincenti, M., Determination of several synthetic cathinones and an amphetamine-like compound in urine by gas chromatography with mass spectrometry. Method validation and application to real cases. *J. Sep. Sci.* **2019,** *42*, 1577-1584.

(22) Woźniak, M. K.; Banaszkiewicz, L.; Wiergowski, M.; Tomczak, E.; Kata, M.; Szpiech, B.; Namieśnik, J.; Biziuk, M., Development and validation of a GC–MS/MS method for the determination of 11 amphetamines and 34 synthetic cathinones in whole blood. *Forensic Toxicol.* **2020**, *38*, 42-58.

(23) Joshi, M.; Cetroni, B.; Camacho, A.; Krueger, C.; Midey, A. J., Analysis of synthetic cathinones and associated psychoactive substances by ion mobility spectrometry. *Forensic Sci. Int.* **2014,** *244*, 196-206.

(24) Peters, J. R.; Keasling, R.; Brown, S. D.; Pond, B. B., Quantification of Synthetic Cathinones in Rat Brain Using HILIC-ESI-MS/MS. *J. Anal. Toxicol.* **2016,** *40*, 718-725.

(25) Williams, M.; Martin, J.; Galettis, P., A Validated Method for the Detection of 32 Bath Salts in Oral Fluid. *J. Anal. Toxicol.* **2017**, *41*, 659-669.

(26) Diestelmann, M.; Zangl, A.; Herrle, I.; Koch, E.; Graw, M.; Paul, L. D., MDPV in forensic routine cases: Psychotic and aggressive behavior in relation to plasma concentrations. *Forensic. Sci. Int.* **2018**, *283*, 72-84.

(27) Garrido, E.; Pla, L.; Lozano-Torres, B.; El Sayed, S.; Martínez-Máñez, R.; Sancenón, F., Chromogenic and fluorogenic probes for the detection of illicit drugs. *ChemistryOpen* **2018**, *7*, 401-428.

(28) García-Fernández, A.; Aznar, E.; Martínez-Máñez, R.; Sancenón, F., New Advances in In Vivo Applications of Gated Mesoporous Silica as Drug Delivery Nanocarriers. *Small* **2020**, *16*, 1902242.

(29) Llopis-Lorente, A.; Lozano-Torres, B.; Bernardos, A.; Martínez-Máñez, R.; Sancenón, F., Mesoporous silica materials for controlled delivery based on enzymes. *J. Mater. Chem. B* **2017**, *5*, 3069-3083.
(30) Giménez, C.; Climent, E.; Aznar, E.; Martínez-Máñez, R.; Sancenón, F.; Marcos, M. D.; Amorós, P.; Rurack, K., Towards chemical communication between gated nanoparticles. *Angew. Chem. Int. Ed. Engl.* **2014**, *53*, 12629-12633.
(31) de Luis, B.; Llopis-Lorente, A.; Rincón, P.; Gadea, J.; Sancenón, F.; Aznar, E.; Villalonga, R.; Murguía, J. R.; Martínez-Máñez, R., An Interactive Model of Communication between Abiotic Nanodevices and Microorganisms. *Angew. Chem. Int. Edi.* **2019**, *58*, 14986-14990.
(32) Garrido, E.; Alfonso, M.; Díaz de Greñu, B.; Lozano-Torres, B.;Parra. M.; Gaviña. P.; Marcos, M.D.; Martínez Mañez, R.; Sancenón, F., Nanosensor for Sensitive Detection of the New Psychedelic Drug 25I-NBOMe. *Chem. Eur. J.* **2020**, *26*, 2813-2816.
(33) Ribes, À.; Aznar, E.; Santiago-Felipe, S.; Xifre-Perez, E.; Tormo-Mas, M. Á.; Pemán, J.; Marsal, L. F.; Martínez-Máñez, R., Selective and Sensitive Probe Based in Oligonucleotide-Capped Nanoporous Alumina for the Rapid Screening of Infection Produced by Candida albicans. *ACS Sensors* **2019**, *4*, 1291-1298.
(34) Oroval, M.; Coll, C.; Bernardos, A.; Marcos, M. D.; Martínez-Máñez, R.; Shchukin, D. G.; Sancenón, F., Selective Fluorogenic Sensing of As(III) Using Aptamer-Capped Nanomaterials. *ACS Appl. Mater. Inter.* **2017**, *9*, 11332-11336.
(35) Aznar, E.; Villalonga, R.; Gimenéz, C.; Sancenón, F.; Marcos, M. D.; Martínez-Máñez, R.; Díez, P.; Pingarrón, J. M.; Amorós, P., Glucose-triggered release using enzyme-gated mesoporous silica nanoparticles. *Chem. Commun.* **2013**, *49*, 6391-6393.
(36) Giménez, C.; Climent, E.; Aznar, E.; Martínez-Máñez, R.; Sancenón, F.; Marcos, M. D.; Amorós, P.; Rurack, K., Towards chemical communication between gated nanoparticles. *Angew. Chem. Int. Ed. Engl*. **2014**, *53*, 12629-33.
(37) Maerten, C.; Garnier, T.; Lupattelli, P.; Chau, N. T. T.; Schaaf, P.; Jierry, L.; Boulmedais, F., Morphogen Electrochemically Triggered Self-Construction of Polymeric Films Based on Mussel-Inspired Chemistry. *Langmuir* **2015**, *31*, 13385-13393.
(38) Beck, J. S.; Vartuli, J. C.; Higgins, J. B.; Schlenker, J. L.; Roth, W. J.; Leonowicz, M. E.; Kresge, C. T.; Schmitt, K. D.; Chu, C. T. W.; Olson, D. H.; Sheppard, E. W.; McCullen, S. B., A new family of mesoporous molecular sieves prepared with liquid crystal templates. *J. Am. Chem. Soc.* **1992,** *114*, 10834.
(39) Cai, Q.; Luo, Z.; Pang, W.; Fan, Y.; Chen, X.; Cui, F., Diluted solution routes to various controllable morphologies of MCM-41 silica with a basic medium. *Chem. Mater*. **2001**, *13*, 258-263.
(40) Paillet-Loilier, M.; Alexandre Cesbron, A.; Le Boisselier, R.; Joanna Bourgine, J.; Debruyne, D., Emerging drugs of abuse: current perspectives on substituted cathinones. *Subst. Abuse Rehabil.* **2014,** *5*, 37-52.
(41) Marusich, J. A.; Antonazzo, K. R.; Wiley, J. L.; Blough, B. E.; Partilla, J. S.; Baumann, M. H., Pharmacology of novel synthetic stimulants structurally related to the "bath salts" constituent 3,4-methylenedioxypyrovalerone (MDPV). *Neuropharmacology* **2014**, *87*, 206-213.
(42) Baumann, M. H.; Partilla, J. S.; Lehner, K. R.; Thorndike, E. B.; Hoffman, A. F.; Holy, M.; Rothman, R. B.; Goldberg, S. R.; Lupica, C. R.; Sitte, H. H.; Brandt, S. D.; Tella, S. R.; Cozzi, N. V.; Schindler, C. W., Powerful Cocaine-Like Actions of 3,4-Methylenedioxypyrovalerone (MDPV), a Principal Constituent of Psychoactive 'Bath Salts' Products. *Neuropsychopharmacol.* **2013**, *38*, 552-562.

SYNOPSIS TOC. A novel bio-inspired nanodevice for the selective and sensitive fluorogenic detection of 3,4-methylenedioxypyrovalerone (MDPV), usually known as Cannibal drug, is presented. The developed nanodevice is based on MCM-41 type mesoporous silica nanoparticles (MSNs). These are loaded with rhodamine B (as a fluorescent reporter) and functionalized on their external surface with a dopamine derivative (which specifically interacts with the recombinant human dopamine transporter, DAT) capping the pores. In the presence of MDPV, DAT detaches from the external surface of the MSNs consequently causing rhodamine B release and allowing drug detection. Thanks to its excellent features, this nanosensor might be useful as a highly selective and sensitive fluorometric probe for the detection of MDPV drug both in saliva and blood plasma samples.